Fractional thermal load in cryogenically cooled Yb:YLF and Yb:YAG lasers

MUHARREM KILINC,[1,2,*] UMIT DEMIRBAS,[1,3,4] JELTO THESINGA,[1] MARTIN KELLERT,[1] FRANZ X. KÄRTNER,[1,2,5] AND MIKHAIL PERGAMENT,[1]

[1]*Center for Free-Electron Laser Science CFEL, Deutsches Elektronen-Synchrotron DESY, Notkestr. 85, 22607 Hamburg, Germany*
[2]*Physics Department, University of Hamburg, Luruper Chaussee 149, 22761 Hamburg, Germany*
[3]*Department of Electrical and Electronics Engineering, Antalya Bilim University, 07190 Dosemealti, Antalya, Turkey*
[4]*Paul Scherrer Institute, Forschungsstrasse 111, 5232 Villigen, Switzerland*
[5]*The Hamburg Centre for Ultrafast Imaging, Luruper Chaussee 149, 22761 Hamburg, Germany*
**muharrem.kilinc@desy.de*

Abstract: We present a method for the direct measurement of fractional thermal load (FTL) in cryogenically cooled laser crystals. The experimental methodology involves characterizing the liquid nitrogen evaporation rate in a dewar containing the laser crystals, allowing for the accurate determination of FTL. The FTL is measured to be 1.7 × quantum defect (QD) for Yb:YLF and 1.5 × QD for Yb:YAG under continuous wave lasing conditions. The measured FTL values are then used to calculate the temperature distribution inside the crystals as a function of pump power, and the simulation results are found to be in very good agreement with the in-situ temperature measurements using contactless optical luminescence thermometry. The method and findings presented in this work hold great potential to benefit laser engineers and scientists working with cryogenic lasers to address and overcome temperature-dependent handicaps.

1. Introduction

The impact of pump-induced heating on laser gain media is a critical consideration that can considerably limit the performance of laser/amplifier systems. This is due to temperature-dependent dynamics such as thermal quenching of fluorescence lifetime [1–3], thermal lensing [4–6], thermally induced stress [7–10], output-mode instabilities [11–13], etc. Hence, an accurate determination of the temperature distribution within laser crystals becomes quite important to overcome these thermal limitations. A key parameter in this context is the fractional thermal load (FTL), representing the ratio of heat load generated to absorbed pump power in the laser gain medium.

Existing approaches to estimate FTL indirectly often rely on observation of the variation of crystal temperature or thermal lensing as a function of absorbed pump power, but these methods require precise knowledge of additional system parameters, such as thermal conductivity, thermo-optic coefficient, and photo-elastic coefficients [14–18]. Direct measurements, including laser calorimetry [19–21] and monitoring the current of the heat sink thermoelectric module [22], offer accurate alternative approaches. However, it is important to emphasize that these methods are only compatible with room temperature measurements.

The amount of fractional thermal load can typically be estimated by studying electron transfer mechanisms between energy levels, such as quantum defect, excited state absorption, auger up-conversion, and thermal quenching of fluorescence [23–26]. However, these mechanisms are not always well-known for all gain media, and specific cases require detailed spectroscopic studies. Even with complete knowledge of energy transitions, it remains challenging to determine which mechanism predominates and to what extent. Consequently, determining the fractional thermal load remains essential.

In this paper, we introduce a novel method for direct measurement of fractional thermal load in cryogenically cooled lasers. Moreover, for the first time, we are reporting the measured FTL values for Yb:YLF and Yb:YAG materials under lasing conditions at cryogenic temperature.

2. Experimental Methodology

Our novel approach to measuring the fractional thermal load is based on the measurement of the liquid nitrogen evaporation rate in the dewar containing the laser crystal. First, the liquid nitrogen evaporation rate of the dewar is characterized as a function of a known heat load, created by a calibrated resistive heating element. Then, during continuous wave (CW) lasing operation, the evaporation rate of the dewar is measured as a function of absorbed pump power for both Yb:YLF and Yb:YAG crystals. One can then directly infer the heat load created by the laser crystals by comparing the measured liquid nitrogen evaporation rate with the earlier curve obtained using the resistive heating element. The variation of the heat load with absorbed pump power is then used to calculate the fractional thermal load induced inside the crystal.

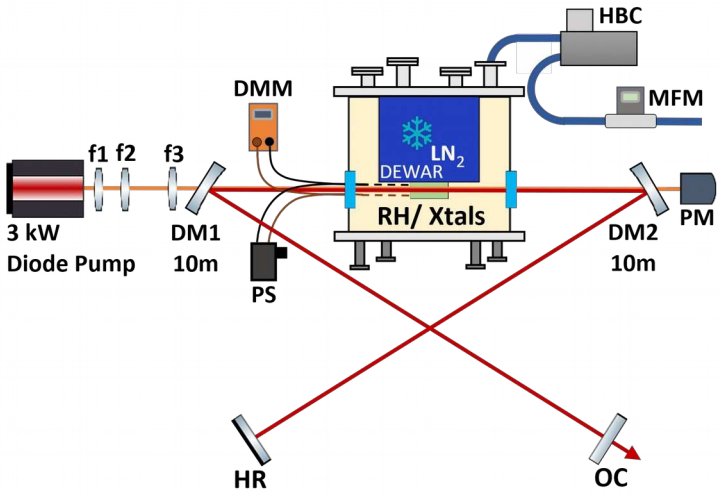

Fig. 1. A schematic of the experimental setup used in fractional thermal load measurements of cryogenic Yb:YLF and Yb:YAG lasers. PS, power source; DMM, digital multimeter; RH, resistive heater; HBC, heating bath circulator; MFM, mass flow meter; f, focusing lens; DM, dichroic mirror; HR, high-reflecting mirror; OC, output coupler; PM, power meter.

Fig. 1 shows the schematic diagram of the setup used for FTL measurements. The dewar used for the experiments is designed and fabricated in house. For the characterization of the evaporation rate of the dewar as a function of heat load, a commercial 200 W cartridge resistive heating element (RH, RS PRO 860-7075, Fig. 2 (b, inset)) is placed into a copper block which mechanically mounted at the same position where the gain medium is placed later, to mimic the crystals' heat load. For better visualization, Fig. 2 shows photos of Yb:YLF crystal indium soldered to the copper heat sink and the mounted resistive heating block, respectively. They are both thermally connected to the cold head of the dewar. The heating element is operated by an adjustable power supply (PS) via a vacuum feedthrough. The voltage applied and resistance response of the heating element are measured simultaneously by a digital multimeter (DMM, Fluke 116) that is connected across the heating element. By using the basic electric power formula ($P=V^2/R$), the power that turns into heat energy is calculated (cable connection losses are negligible). While the heating

element is powered, it is actively cooled by liquid nitrogen (LN_2). Subsequently LN_2 evaporates and leaves the dewar over an exhaust pipe in gas form. The exhaust of the dewar is connected to a mass flow meter (MFM, Aalborg Instruments DPM47) measuring the gas flow (evaporation rate). Since the evaporation temperature of LN_2 is 77 K, it freezes the MFM. Therefore, a heating bath circulator (HBC, Thermo Scientific™ 1561071) is placed between the mass flow meter and dewar to increase and stabilize the temperature of the gas that reaches to MFM around room temperature.

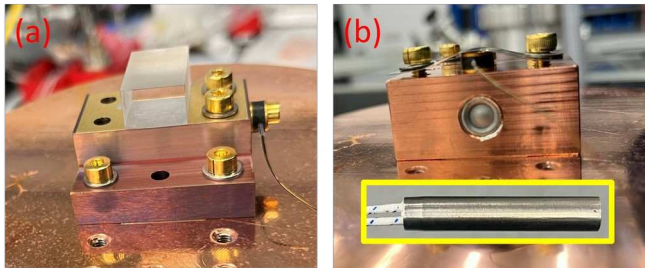

Fig. 2. (a) A picture of the Yb:YLF crystal that is indium soldered to the copper heat sink. The crystal assembly is connected to the cold head of the dewar. (b) A picture of the resistive heating block mechanically mounted to the cold head of the dewar. The inset shows a picture of the 200 W cartridge resistive heating element used in the experiments.

The setup used for the CW lasing experiments is also shown schematically in Fig. 1. The Yb-doped YLF crystal has a 1 % doping concentration, and it is 20 mm long, 15 mm wide, and 10 mm thick. Similarly, the Yb-doped YAG crystal also has 1 % doping concentration, and it is 23 mm long, 15 mm wide, and 5 mm thick. The Yb:YLF crystal has 3 mm long undoped endcaps on both ends, and hence the total crystal length is 26 mm. The Yb:YAG crystal has a 3 mm undoped cap on its front side only, and therefore has a total length of 26 mm. A 960 nm and a 940 nm fiber-coupled diode system providing up to 3 kW of output power are used as the pump source for Yb:YLF and Yb:YAG crystal, respectively. To focus the pump beam into the crystals, we utilize a f1-f2 telescope to image the fiber mode. But due to the small working range of the f1-f2 telescope, another 300 mm focal length lens (f3) is necessary to re-image the pump beam with a beam diameter of 2.1 mm inside the crystal. A standard X-type cavity is employed that consists of two curved high reflecting mirrors with a radius of curvature (ROC) of 10 m (DM1, DM2), a flat-end high reflector (HR), and a flat output coupler (OC). The high reflector and output coupler arm lengths are both set to 80 cm with approximately 60 cm separation between DM1 and DM2. Both dichroic pump mirrors, DM1 and DM2, have anti-reflection coatings for the 940-960 nm range. All three high reflectors in the laser cavity, DM1, DM2, and HR, have reflective coatings covering the spectral range 990-1040 nm. For output coupling 40 % and 25 % transmitting OCs in the range of 990-1040 nm are used for Yb:YLF and Yb:YAG, respectively.

As we are interested in measuring the primary heat load that is responsible for internal heating of the laser gain element, we tried to minimize all secondary heat sources. First of all, the inner walls of the dewar are coated with a highly absorptive material that absorbed more than 98 % of light in the range of 400-1100 nm. The aim is to avoid any stray light (spontaneous emission or scattered pump light) reflecting from the inner walls and hitting back to the cold head of the LN_2 tank. If stray light hits back to the cold head, it might create an extra heat load and consume extra LN_2, and this could result in an error in measuring the real fractional thermal load of the system. Additionally, the absorbed energy in the dewar walls is removed by a water chiller connected to the outer chamber of the dewar. The cold head used is made of copper which has a reflectivity above 80 % in the infrared wavelength

range [27]. The setup is similar to what was used in our previous lasing/and amplification studies [28–30], and enables us to understand thermal load limitations for further power scaling of rod-based cryogenic Yb-doped YLF and YAG systems. As a side note, the absorber coatings on the inner walls and reflective coatings on the cold head are not perfect (100 %), so the measurements give an upper limit for the fractional thermal load (FTL). The actual FTL may be slightly lower but not higher. In the next section we show that the thermo-mechanical simulations show good agreement with measurements, supporting the claim that the upper limit is close to the real value of the FTL.

3. Experimental results and discussion

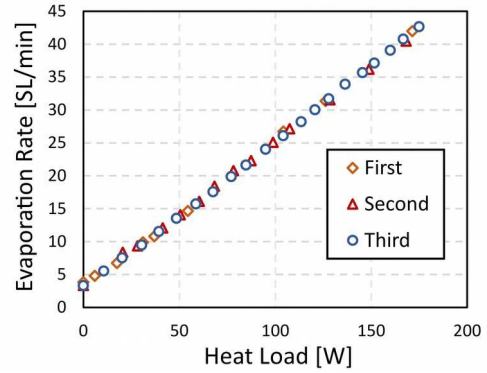

Fig. 3. Measured evaporation rate of the dewar system as a function of the applied heat load via the resistive heater.

Fig. 3 shows the measured liquid nitrogen (LN_2) evaporation rate of the dewar as a function of known heat load applied to the crystal via the resistive heater. The measurement has been repeated three times at different dates to confirm repeatability of the measurement. As can be seen, measurements agree very well with each other. As expected, the liquid nitrogen evaporation rate is linearly increasing with heat load for at least up to 170 W. This confirms that the system is still rather far away from Leidenfrost effects starting at the surface [31]. Leidenfrost effects occur when a liquid comes into contact with a surface that is considerably hotter than its boiling point, forming a vapor layer that insulates it from direct contact with the surface. Since the system is not reaching temperatures high enough to induce this phenomenon, effective cooling can be achieved at the dewar liquid nitrogen contact point. Note that the dewar consumes about 3 standard liters per minute (SL/min) of liquid nitrogen, without any heat load, and the liquid nitrogen consumption increases around 0.23 SL/min per W.

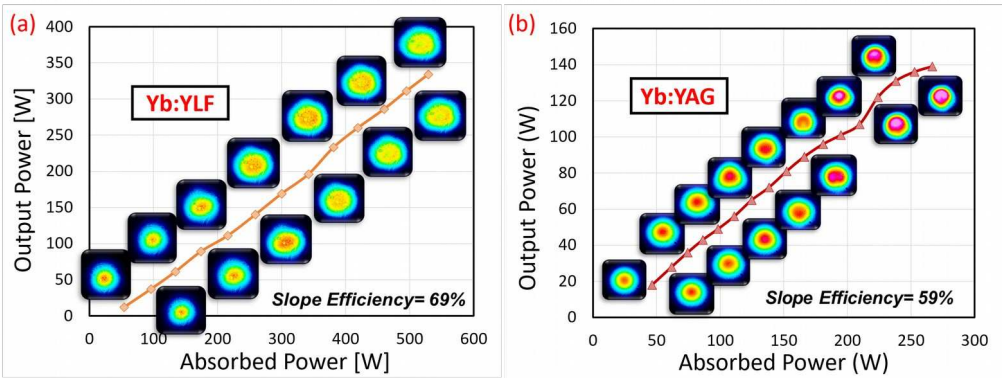

Fig. 4. Measured CW laser performance of the cryogenically cooled (a) Yb:YLF and (b) Yb:YAG lasers using output couplers with a transmission of 40 % and 25 %, respectively. The insets display the near-field beam profiles of the laser beams at each data point. The slope efficiencies for the Yb:YLF and Yb:YAG lasers are calculated as 69 % and 59 %, respectively.

Fig. 4 shows the summary of continuous wave laser performance of the cryogenically cooled Yb:YLF and Yb:YAG lasers, respectively. Since our previous studies demonstrated that the best continuous wave performance was achieved with output couplers of 40 % for Yb:YLF and 25 % for Yb:YAG, we have chosen to utilize them in this study as well [29,30]. With these output coupling values, we observed a lasing threshold of around 30 W and 60 W for Yb:YLF and Yb:YAG, respectively. For Yb:YLF, the laser produced a maximum CW output power of 330 W around 1019 nm at an absorbed pump power of 530 W, and the estimated slope efficiency is 69 %. As a side note we have observed lasing at 995 nm up to 100 W of absorbed power. Above that level, the lasing wavelength shifts to 1019 nm due to temperature induced changes in the gain spectrum (a detailed discussion of this effect can be found in our previous studies [29,30,32]). For the case of Yb:YAG, the laser produced a maximum CW output power of 140 W around 1030 nm at an absorbed pump power of 270 W, and the estimated slope efficiency is 59 %. The reason for the lower absorbed power levels compared to the Yb:YLF system is that the thermal lens becomes too dynamic above 250 W absorption, and stable continuous wave lasing was not feasible. The thermal lensing effects are visibly evident in the insets of Fig. 4, by the displayed near-field output beam profiles at each data point. For Yb:YAG, the center of the output beam profile becomes brighter, and the beam size becomes smaller due to thermal lensing, and instability arises above 250 W of absorbed pump power. On the other hand, the Yb:YLF output becomes multi-mode at increased power level, but laser was still stably operating thanks to the much smaller overall thermal lensing in Yb:YLF [6,30]. Hence, we could even go higher pump power levels for Yb:YLF [29] but without any additional benefit for the FTL measurements since Yb:YLF demonstrated a linear output power dependency on absorbed power.

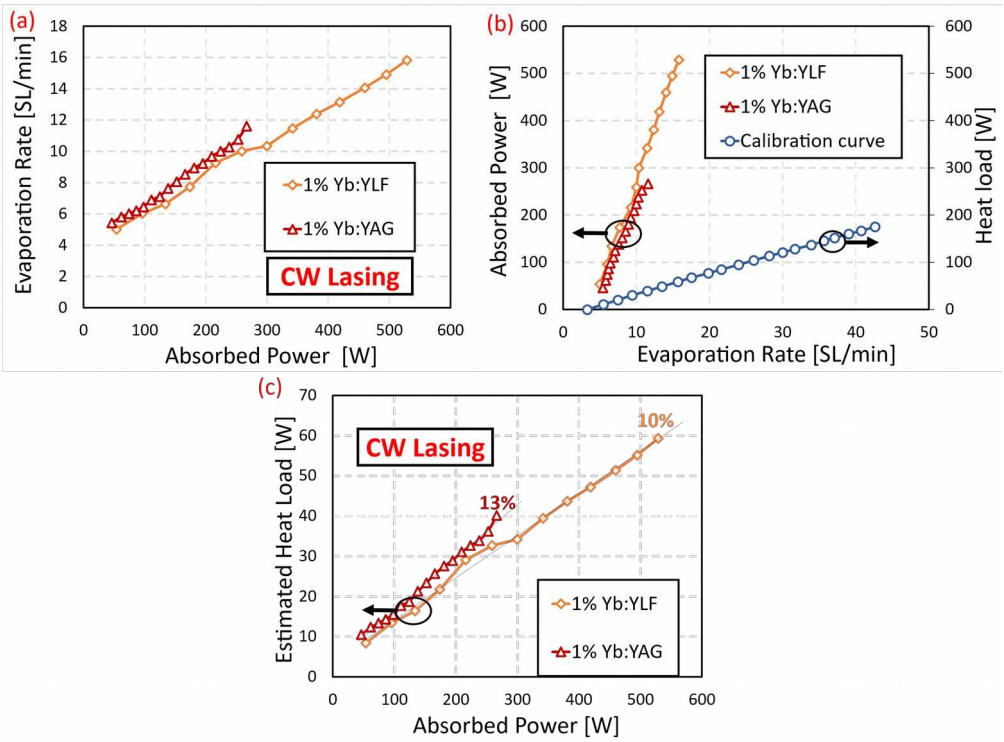

Fig. 5. (a) Measured evaporation rates of cryogenic Yb:YLF and Yb:YAG systems during CW lasing operation as a function of absorbed pump power. (b) Measured relationship between absorbed pump power (on the left axis) and heat load (on the right axis) as a function of evaporation rate. (c) Estimated heat load as a function of absorbed power for the CW cryogenically cooled Yb:YLF and Yb:YAG lasers.

Employing the same methodology utilized in the dewar characterization with the heating element, the evaporation rate of the liquid nitrogen (LN_2) as a function of the absorbed pump power for continuous wave (CW) Yb:YLF and Yb:YAG lasers are measured and shown in Fig. 5 (a). Even though there are small fluctuations in the evaporation rates for both lasers, we observe that they both have a linear trend with respect to the absorbed pump power. The common point in the laser measurements and the reference heating element measurements is the evaporation rate. Therefore, we can directly infer the heat load deposited in the crystals as a function of absorbed pump power as shown in Fig. 5 (b). Then the variation of the heat load with absorbed pump power is used to calculate the fractional thermal load induced inside the crystals. For instance, to estimate the heat load for Yb:YLF at an absorbed power of 300 W, we first follow the curve representing Yb:YLF and find the evaporation rate corresponding to the 300 W absorbed power, which is approximately 10 SL/min. Then, by using the calibration curve we check the heat load that corresponds to a 10 SL/min evaporation rate on the right-hand side of the graph. This procedure results in an estimated heat load for Yb:YLF of approximately 35 W at an absorbed power of 300 W. This principle is followed to calculate the estimated heat load as a function of absorbed power for both lasers and the final characteristic is shown in Fig. 5 (c). Similar to the previous curves, the estimated heat load also has a linear dependence on absorbed pump power. Finally, by linear fitting, the fractional thermal loads (slopes of the trends) are calculated as 10 % for Yb:YLF and 13 % for Yb:YAG under lasing conditions at cryogenic temperature. There are different contributions to FTL, but the basic contribution in Yb-systems is the quantum defect (QD). In our lasing cavity, the quantum defect for Yb:YLF (pumped at 960 nm, lasing at 1019 nm) and Yb:YAG (pumped at 940 nm, lasing at 1030 nm) is around 5.8 % and 8.7 %, respectively. Hence the estimated FTL is 1.7 and 1.5 times the quantum defect for Yb:YLF and Yb:YAG, respectively. We believe that the extra heat load that is generated beyond the quantum defect is a result of undesired effects such as radiation trapping and impurity-induced nonradiative decay [33,34]. Overall, the measured FTL for Yb:YAG in this work is in relatively good agreement with the earlier data presented by T. Y. Fan at room temperature [21].

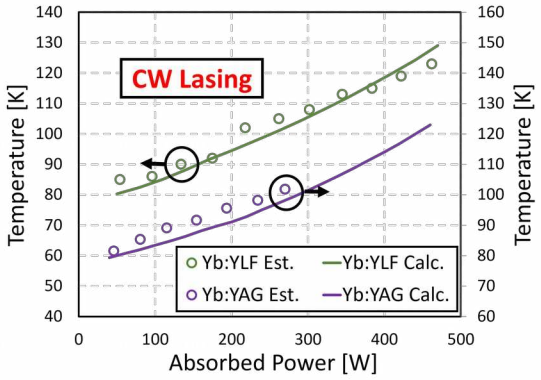

Fig. 6. Measured (open marks) and calculated (solid lines) temperature of cryogenically cooled Yb:YLF and Yb:YAG lasers as a function of absorbed pump power during CW lasing operation. The calculation has been performed for a fractional thermal load (FTL) of 1.7 and 1.5 times the quantum defect (QD) for Yb:YLF and Yb:YAG, respectively.

Moreover, to confirm our FTL findings, we have compared the estimated and calculated average temperatures of the crystals. First, the optical contactless temperature probing method

based on variation of fluorescence spectra with temperature [35,36] is used to estimate the average temperature of the crystals at different absorbed power levels for cryogenic Yb:YAG and Yb:YLF lasers. Then, we calculated the average temperature in both crystals as a function of the absorbed power at cryogenic temperatures. Finally, Fig. 6 compares the estimated and calculated outcomes. Open marks are the estimated temperature by the contactless optical temperature probing methods while solid lines represent the calculations by assigning FTL as 1.7 × QD and 1.5 × QD for Yb:YLF and Yb:YAG, respectively. Fig. 6 shows that our detailed thermomechanical calculations of the crystal temperature using the measured FTL values are in excellent agreement with the estimated temperatures of the crystals, confirming the validity of the measured FTLs for cryogenically cooled Yb:YLF and Yb:YAG crystals under continuous wave extraction. As a side note, for the temperature calculations, the model described in one of our previous studies [6] is utilized, with additional details provided in the appendix below.

4. Conclusion

We have presented a method for the direct measurement of the fractional thermal load (FTL) under lasing conditions at cryogenic temperatures. FTLs for cryogenically cooled Yb:YLF and Yb:YAG materials are measured under lasing conditions for the first time as 1.7 and 1.5 times the quantum defect, respectively. The presented method and the reported FTL values are anticipated to facilitate the laser community in predicting heat load-dependent dynamics and enhancing the performance of cryogenically cooled Yb-doped YLF and YAG-based solid-state lasers and amplifiers.

Appendix

For the temperature calculations, the model described in one of our previous studies [6] is employed. For more details, we refer to the paper. Table 1 provides the related parameters used for simulation of the thermal behavior of Yb:YLF and Yb:YAG crystals under continuous wave extraction.

Table 1. Parameters of the fiber-coupled pumped 1% Yb-doped YLF and YAG crystals for simulations. T in equations stands for temperature in Kelvin.

Parameter	Symbol	Yb:YLF	Yb:YAG
Absorbed Pump Power	$P_{¿¿¿}$	$0 ¿ 600\,W$	
Pump Beam Waist	w_0	$1.05\,mm$	
Pump Beam Quality Factor	M^2	220	
Super Gaussian Order of Pump	N	20	
Pump Wavelength	λ_p	$960\,nm$	$940\,nm$
Doping Concentrations	N_{dop}	1 %	1 %
Specific Heat Capacity	C_p	$300\,J/(kg.K)$	$150\,J/(kg.K)$
Density	Rho	$3950\,kg/m^3$	$4560\,kg/m^3$
Refractive Index	n	1.4485	

Fractional Thermal Load	FTL	$1.7 \times QD$	$1.5 \times QD$
Doped Crystal Length	L_{doped}	$20\,mm$	$23\,mm$
Undoped Cap Length	$L_{undoped}$	$2 \times 3\,mm$	$3\,mm$
Crystal Height	D	$10\,mm$	$5\,mm$
Crystal Width	W	$15\,mm$	$15\,mm$
Thermal Conductivity	k	$14300\,T^{-1.41}\,W/(m.K)$ (E//a $21200\,T^{-1.42}$ W/(m.K) (E// [39]	$13414\,T^{-1.3}\,W/(m.K$

Funding. Deutsche Forschungsgemeinschaft (390715994); European Research Council (609920).

Disclosures. The authors declare no conflicts of interest.

Data availability. Data underlying the results presented in this paper are not publicly available at this time but may be obtained from the authors upon reasonable request.

References

1. J. R. Lakowicz, "Quenching of Fluorescence," Principles of Fluorescence Spectroscopy 257–301 (1983).
2. M. Stalder, M. Bass, and B. H. T. Chai, "Thermal quenching of fluorescence in chromium-doped fluoride laser crystals," Journal of the Optical Society of America B **9**(12), 2271 (1992).
3. S. Okuyucu, J. Thesinga, H. Tanaka, Y. Ozturk, F. X. Kärtner, M. Pergament, and U. Demirbas, "Temperature dependence of the emission cross-section and fluorescence lifetime in Cr:LiCAF, Cr:LiSAF, and Cr:LiSGaF between 78 K and 618 K," Opt Mater Express **13**(5), 1211 (2023).
4. B. Neuenschwander, R. Weber, and H. P. Weber, "Determination of the Thermal Lens in Solid-State Lasers with Stable Cavities," IEEE J Quantum Electron **31**(6), 1082–1087 (1995).
5. E. Anashkina and O. Antipov, "Electronic (population) lensing versus thermal lensing in Yb:YAG and Nd:YAG laser rods and disks," Journal of the Optical Society of America B **27**(3), 363 (2010).
6. M. Kilinc, U. Demirbas, J. B. Gonzalez-Diaz, J. Thesinga, M. Kellert, G. Palmer, F. X. Kärtner, and M. Pergament, "Thermal and population lensing of Yb:YLF at cryogenic temperature," Opt Mater Express **13**(11), 3200 (2023).
7. J. E. Marion, "Fracture of solid state laser slabs," J Appl Phys **60**(1), 69–77 (1986).
8. Y. Matsuoka, "Laser-induced damage to semiconductors," J Phys D Appl Phys **9**(2), 215–224 (1976).
9. Y. F. Chen, Y. P. Lan, and S. C. Wang, "High-power diode-end-pumped Nd:YVO4 laser: Thermally induced fracture versus pump-wavelength sensitivity," Appl Phys B **71**(6), 827–830 (2000).
10. A. K. Cousins, "Temperature and Thermal Stress Scaling in Finite-Length End-Pumped Lasers Rods," IEEE J Quantum Electron **28**(4), 1057–1069 (1992).
11. C. Jauregui, T. Eidam, H.-J. Otto, F. Stutzki, F. Jansen, J. Limpert, and A. Tünnermann, "Temperature-induced index gratings and their impact on mode instabilities in high-power fiber laser systems," Opt Express **20**(1), 440 (2012).
12. C. Jauregui, H.-J. Otto, N. Modsching, J. Limpert, and A. Tünnermann, "Recent progress in the understanding of mode instabilities," Fiber Lasers XII: Technology, Systems, and Applications **9344**(March 2015), 93440J (2015).

13. W.-W. Ke, X.-J. Wang, X.-F. Bao, and X.-J. Shu, "Thermally induced mode distortion and its limit to power scaling of fiber lasers," Opt Express **21**(12), 14272 (2013).
14. A. Sennaroglu, "Experimental determination of fractional thermal loading in an operating diode-pumped Nd:YVO_4 minilaser at 1064 nm," Appl Opt **38**(15), 3253 (1999).
15. T. S. Chen, V. L. Anderson, and O. Kahan, "Measurements of Heating and Energy Storage in Diode-Pumped Nd:YAG," Optics InfoBase Conference Papers **26**(0018), 295–300 (1989).
16. A. McInnes, J. Richards, K. W. DeLong, D. N. Fittinghoff, and R. Trebino, "Thermal effects in a coplanar-pumped folded-zigzag slab laser," IEEE J Quantum Electron **32**(7), 1243–1264 (1996).
17. Y.-F. Chen and H.-J. Kuo, "Determination of the thermal loading of diode-pumped Nd:YVO_4 by use of thermally induced second-harmonic output depolarization," Opt Lett **23**(11), 846 (1998).
18. Y. Wang, W. Yang, H. Zhou, M. Huo, and Y. Zhen, "Temperature dependence of the fractional thermal load of Nd:YVO_4 at 1064 nm lasing and its influence on laser performance," Opt Express **21**(15), 18068 (2013).
19. A. J. Ramponi and J. A. Caird, "Fluorescence quantum efficiency and optical heating efficiency in laser crystals and glasses by laser calorimetry," J Appl Phys **63**(11), 5476–5484 (1988).
20. B. Comaskey, B. D. Moran, G. F. Albrecht, and R. J. Beach, "Characterization of the Heat Loading of Nd-Doped YAG, YOS, YLF, and GGG Excited at Diode Pumping Wavelengths," IEEE J Quantum Electron **31**(7), 1261–1264 (1995).
21. T. Y. Fan, "Heat Generation in Nd:YAG and Yb: YAG," IEEE J Quantum Electron **29**(6), 1457–1459 (1993).
22. Y. T. Wang and R. H. Zhang, "Comprehensive analysis of heat generation and efficient measurement of fractional thermal loading in a solid-state laser medium," Laser Phys **27**(12), (2017).
23. F. Sanchez and A. Kellou, "Laser dynamics with excited-state absorption," Journal of the Optical Society of America B **14**(1), 209 (1997).
24. G. Blasse, "Thermal quenching of characteristic fluorescence," J Chem Phys **51**(8), 3529–3530 (1969).
25. S. A. Payne, G. D. Wilke, L. K. Smith, and W. F. Krupke, "Auger upconversion losses in Nd-doped laser glasses," Opt Commun **111**(3–4), 263–268 (1994).
26. U. Demirbas, "Cr:Colquiriite Lasers: Current status and challenges for further progress," Prog Quantum Electron **68**(August), 100227 (2019).
27. J. F. Ready, *Industrial Applications of Lasers* (Elsevier, 1997).
28. U. Demirbas, M. Kellert, J. Thesinga, Y. Hua, S. Reuter, M. Pergament, and F. X. Kärtner, "Highly efficient cryogenic Yb:YLF regenerative amplifier with 250 W average power," Opt Lett **46**(16), 3865 (2021).
29. M. Kellert, U. Demirbas, J. Thesinga, S. Reuter, M. Pergament, and F. X. Kärtner, "High power (>500W) cryogenically cooled Yb:YLF cw-oscillator operating at 995 nm and 1019 nm using E//c axis for lasing," Opt Express **29**(8), 11674 (2021).
30. U. Demirbas, M. Kellert, J. Thesinga, S. Reuter, F. X. Kärtner, and M. Pergament, "Advantages of YLF host over YAG in power scaling at cryogenic temperatures: direct comparison of Yb-doped systems," Opt Mater Express **12**(7), 2508 (2022).
31. J. G. Leidenfrost, *A Track about Some Qualities of Common Water* (Carolyn SE Wares, 1966), **9**.
32. U. Demirbas, J. Thesinga, M. Kellert, F. X. Kärtner, and M. Pergament, "Detailed investigation of absorption, emission and gain in Yb:YLF in the 78–300 K range," Opt Mater Express **11**(2), 250 (2021).
33. D. V. Seletskiy, S. D. Melgaard, R. I. Epstein, A. Di Lieto, M. Tonelli, and M. Sheik-Bahae, "Local laser cooling of Yb:YLF to 110 K," Opt Express **19**(19), 18229 (2011).

34. E. S. de L. Filho, G. Nemova, S. Loranger, and R. Kashyap, "Laser-induced cooling of a Yb:YAG crystal in air at atmospheric pressure," Opt Express **21**(21), 24711 (2013).
35. U. Demirbas, J. Thesinga, M. Kellert, F. X. Kärtner, and M. Pergament, "Comparison of different in situ optical temperature probing techniques for cryogenic Yb:YLF," Opt Mater Express **10**(12), 3403 (2020).
36. U. Demirbas, J. Thesinga, M. Kellert, S. Reuter, F. X. Kärtner, and M. Pergament, "Error analysis of contactless optical temperature probing methods for cryogenic Yb:YAG," Appl Phys B **127**(8), 1–10 (2021).
37. T. Radhakrishnan, "Temperature variation of the refractive index of lithium fluoride," Proceedings of the Indian Academy of Sciences - Section A **31**(4), 224–228 (1950).
38. D. E. Zelmon, D. L. Small, and R. Page, *Refractive-Index Measurements of Undoped Yttrium Aluminum Garnet from 0.4 to 5.0 m* (1998).
39. R. L. Aggarwal, D. J. Ripin, J. R. Ochoa, and T. Y. Fan, "Measurement of thermo-optic properties of $Y_3Al_5O_{12}$, $Lu_3Al_5O_{12}$, $YAlO_3$, $LiYF_4$, $LiLuF_4$, BaY_2F_8, $KGd(WO_4)_2$, and $KY(WO_4)_2$ laser crystals in the 80–300K temperature range," J Appl Phys **98**(10), (2005).